Formation of autoionizing states of Ne in collisions with surfaces

G. Zampieri, F. Meier,* and R. Baragiola
Centro Atómico Bariloche, Comisión Nacional de Energía Atómica, 8400 Bariloche, Argentina
and Instituto Balseiro, Comisión Nacional de Energía Atómica y Universidad Nacional de Cuyo, 8400 Bariloche, Argentina
(Received 14 January 1983)

We have measured energy spectra of electrons resulting from collisions of 0.4—5.0-keV Ne^+ with solid targets of Mg, Al, and Si. We found only two peaks, in the electron-energy range 20—30 eV, corresponding to the autoionization of the Ne^{**} $2p^4(^3P,^1D)3s^2$ states. Unlike the spectra from gas-phase collisions, the peak with the ^3P core is the most intense. We interpret our results with a model involving reflection and excitation of the projectile in its collision with the surface. The excitation mechanism is similar to that of gas-phase collisions; new effects appear due to the continuum of electronic states in the solid.

I. INTRODUCTION

Electron spectroscopy of heavy-ion—atom collisions in the gas phase has received much attention in the last years. This interest is owed mainly to the peculiar features presented by this kind of collision, and the possibility of a simple interpretation of the results based on the electron-promotion model.

In contrast with this extensive work, few papers have appeared on electron spectroscopy of heavy-ion collisions with atoms in solids. This kind of collision offers the tempting possibility of large signals due to the high concentration of target atoms, but, on the other hand, many new effects arise, characteristic of the solid phase. Nevertheless, existent results[1,2] suggest that the projectile excitation is little affected by the solid, and retains the atomic nature of gas-phase processes. The study of these excitations by means of electron spectroscopy reveals important features of the atom-solid system; it also supplements the knowledge of a wide variety of phenomena occurring in atom-solid collisions: target excitation, secondary electron emission, secondary ion emission, backscattering of projectiles, etc.

In this paper we report measurements on projectile excitation in collisions of 0.4—5-keV Ne^+ with clean surfaces of Mg, Al, and Si. Throughout this study, we compare our results with those of collisions in the gas-phase, finding strong similarities and differences.

The apparatus and some experimental techniques used in this work are described in Sec. II. In Sec. III we present our results, which are interpreted in Sec. IV. Finally, we summarize our conclusions in Sec. V.

II. EXPERIMENTAL DETAILS

A. Apparatus

The experimental data were taken in a conventional ultrahigh vacuum system routinely operated at a base pressure less than 3×10^{-11} Torr. With differential pumping we prevented pressure rises in the target chamber while admitting neon gas to the ion gun. The pressure in the target chamber during ion bombardment was always less than 10^{-8} Torr.

An electron-bombardment-type ion gun produced the Ne^+ ions; they were mass analyzed by means of a Wien filter and deflected electrostatically onto the target to separate them from possible neutral atoms in the beam.

Electrons ejected during ion bombardment were energy analyzed with a hemispherical electrostatic analyzer working, with preretardation of the electrons, at an energy resolution of 0.5%. In this operation mode, the transmission function is proportional to the electron energy. The spectra to be shown are corrected for this function except when indicated.

The geometrical disposition of the solid target, the ion gun, and the analyzer is shown in Fig. 1; the angle between the ion-gun direction and the analyzer direction is fixed (47°); the samples were placed at angles $\psi=15°$, 45°, and 65°.

B. Samples

We used polycrystalline samples of Be, Mg, Al, and amorphized Si; they were cleaned by sputtering with low-energy Ar^+ ions. The cleanliness of the surfaces was monitored by means of electron-induced Auger-electron

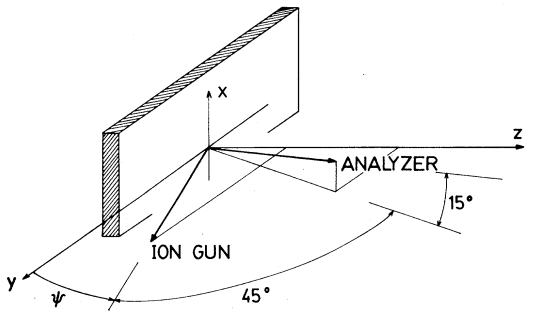

FIG. 1. Geometry of the experiment: z is the direction normal to the surface; the angle between the ion gun and the analyzer directions is fixed (47°). Samples of Be, Mg, Al, and Si were placed at angles $\psi=15°$, 45°, and 65°.

spectroscopy. The surface concentration of the main contaminants remaining (oxygen and implanted argon), was estimated to be less than 2% and 1% for Mg and Al, respectively. In the case of Si no oxygen signal was detected and the implanted argon concentration was estimated to be 1.5%, whereas for Be the oxygen and argon concentration were less than 0.3% and 2.5%, respectively.

C. Work-function measurements

In order to compare our electron-energy spectra with those of gas-phase collisions, the electron kinetic energy K must be referred to the vacuum level of the target; with our hemispherical electrostatic analyzer this energy is (see Fig. 2 with $V_p=0$):

$$K=(eR+HV_{\text{anal}})+W_{\text{sp}}-W_t\ , \tag{1}$$

where e is the electron charge, R the retardation voltage prior to analysis, HV_{anal} the analyzer pass energy, and W_{sp} (W_t) the work function of the spectrometer (target).

To determine the work function of the spectrometer we accelerated a beam of electrons onto the target through an accurately known potential, and observed the most probable energy of the elastically reflected electrons.[3] This procedure is expected to be accurate to within 0.1 eV.

To determine the work function of the target we measured electron-energy spectra with the target at a negative potential V_p; Eq. (1) now becomes (see Fig. 2)

$$K=(eR+HV_{\text{anal}})+W_{\text{sp}}-W_t-eV_p\ .$$

Electrons with $K=0$, i.e., electrons which escape from the solid with energy just above its vacuum level, are easily identified at the low-energy edge of these spectra. We then get

$$W_t=(eR+HV_{\text{anal}})_{K=0}+W_{\text{sp}}-eV_p\ .$$

With this method we measured the work functions of the Mg, Al, and Si samples obtaining 3.68, 4.25, and 4.78 eV, respectively, with an estimated uncertainty of ± 0.15 eV, in good agreement with published values.[4]

III. RESULTS

A. Peak intensities

Figure 3 shows electron-energy spectra taken under 1-keV Ne^+ bombardment of Mg, Al, and Si samples

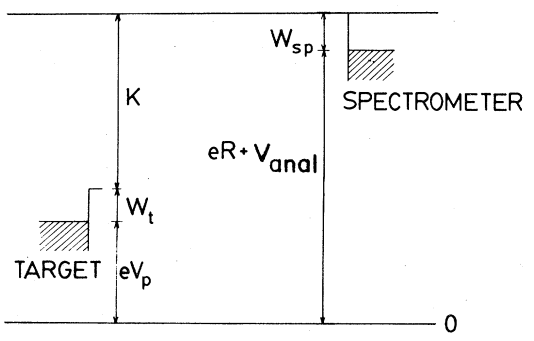

FIG. 2. Electron-energy diagram appropriate to work-function measurements.

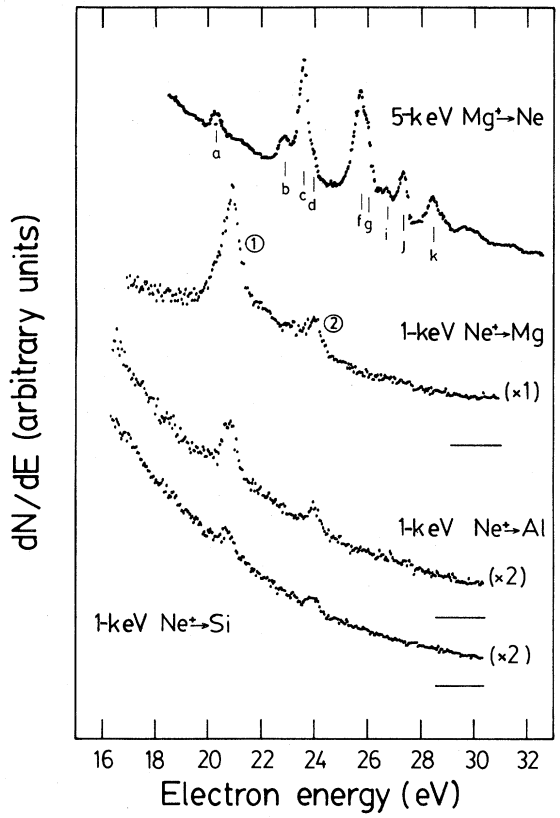

FIG. 3. Electron-energy spectra from collisions of Mg^+ with gaseous Ne [from Andersen and Olsen (Ref. 5)] and Ne^+ with solid targets, $\psi=45°$ (this work). All lines belong to neon autoionizing states $2p^4nln'l'$. Stronger lines in the Mg^+-Ne spectrum c, f, g, j, and k have a $2p^4(^1D)$ core state; the weaker lines a, b, d, and i have a $2p^4(^3P)$ core state. Only two lines appear in the Ne^+-Mg, Al, and Si spectra, which are labeled 1 and 2.

($\psi=45°$). Also included for comparison is a spectrum from gas-phase collision experiments. Our spectra exhibit two prominent atomiclike peaks, which we have labeled peak 1 (low-energy peak) and peak 2 (high-energy peak). Both were identified in a previous investigation[2] (to be referred to as *I*) to correspond to the neon autoionizing states $2p^4(^3P)3s^2$ and $2p^4(^1D)3s^2$, respectively. It is seen that their intensities decrease with the atomic number of the target Z_2.

In order to study the shape of these peaks we subtracted the background on which they are superimposed. As in *I*, this was done by fitting a function of the form $N(E)=B/(E-E_0)^n+D$ to the low- and high-energy sides of the spectra, where B, E_0, D, and n are the fitting constants.

Since a strong increment of the background occurs with increasing projectile energy, the peak to background ratios approach zero as the Ne^+ energy increases. This establishes an upper limit to the projectile energy above which the peaks are not discernible. In the case of Mg and Al targets this limit is ~ 3.5 keV for $\psi=45°$ and higher than 5 keV for $\psi=15°$. A special case is that of the Si target with $\psi=45°$, where the high threshold energy for excita-

tion ($\sim$0.7 keV) and the low value of the upper limit in energy ($\sim$2 keV) severely reduce the working range.

Figure 4 shows the ratio of the intensities of peak 2 to peak 1, I_2/I_1, as a function of incident Ne^+ velocity for two values of the incidence angle ψ. The intensity of each peak was estimated as the product of the height of the peak by its full width at half maximum (FWHM). The ratios increase with the incident Ne^+ velocity and decrease with ψ.

Another much weaker structure at 31 eV was observed with Mg targets. We did not observe any peaks during Ne^+ bombardment of Si at $\psi=65°$, and of Be at $\psi=15°$ and 45°.

B. Peak widths

Figures 5 and 6 show electron-energy spectra taken during Ne^+ bombardment of Al surfaces at $\psi=15°$ and 45°. It is observed that the peak shapes are similar at incident Ne^+ energies smaller than $\sim$1.5 keV. At larger impact energies, the peak shapes are clearly different, showing a pronounced broadening in the low-energy side, in the spectra with the target at $\psi=15°$. This was also seen with Mg targets.

In Fig. 7 we plotted the FWHM of the peaks from samples at $\psi=45°$ versus the incident Ne^+ velocity. Figure 8 shows a similar plot, but for the low-energy half-width at half maximum (HWHM) of the peaks from samples at

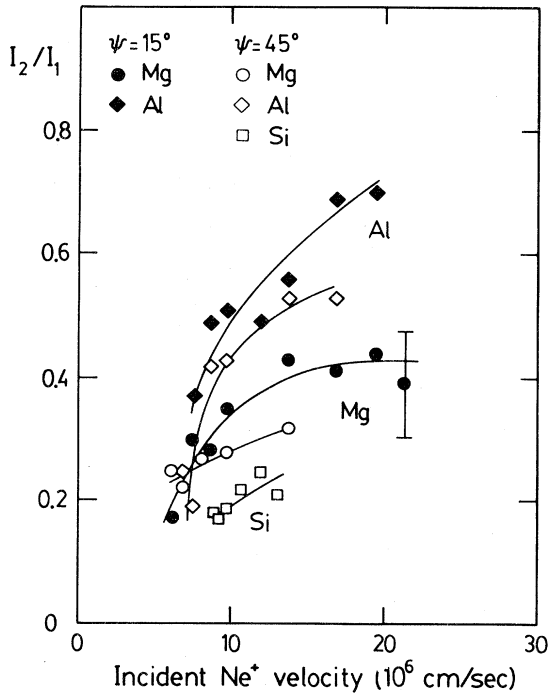

FIG. 4. Ratio of the intensities of peak 2 to peak 1 vs the incident Ne^+ velocity. Each intensity has been estimated as the product of the peak height by the FWHM. Since peak labeled 2 appears deformed in the spectra from Ne^+-Mg ($\psi=15°$) at incident Ne^+ velocities greater than 10^7 cm/sec, we estimated the ratio of the intensities as the quotients of the peak heights. Lines are drawn to guide the eye and have no other meaning.

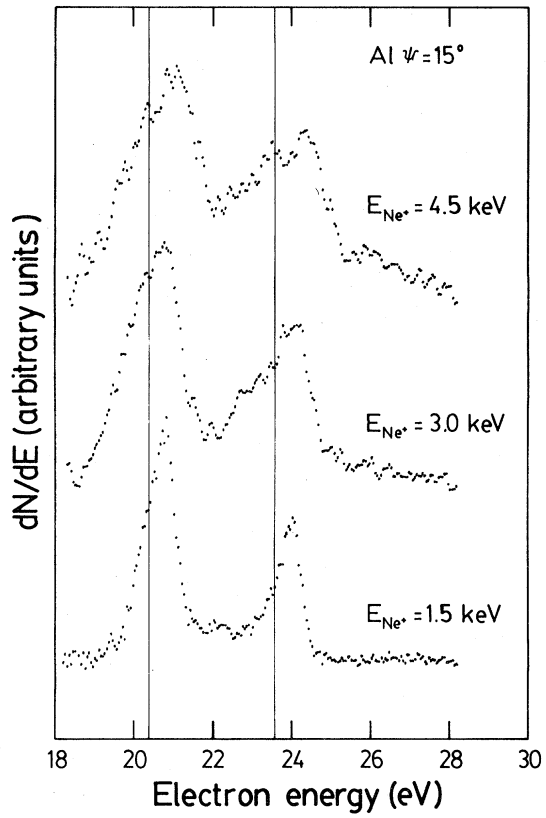

FIG. 5. Electron-energy spectra (after background subtraction) from collisions of 1.5-, 3.0-, and 4.5-keV Ne^+ with Al surfaces. Incidence angle $\psi=15°$. Light vertical lines indicate the energies of autoionization in free space.

$\psi=15°$. It is observed in Figs. 7 and 8 that the peak widths decrease with increasing Z_2.

C. Peak positions

In Fig. 9 we plotted the peak positions versus the incident Ne^+ velocity. A shift of 0.3—0.4 eV is observed to energies higher than the energy of autoionization in free space (20.35 and 23.55 eV for peaks 1 and 2, respectively[5]); the general trend of this shift is to increase with projectile velocity, irrespective of the sample orientation.

IV. DISCUSSION

In *I* it was concluded that the peaks in our spectra originate in the decay of the autoionizing states $2p^4(^3P,^1D)3s^2$ of neon atoms moving outside the surface. The whole process involves reflection and excitation of the projectile in its collision with the solid, and the subsequent deexcitation when it escapes from the surface. The purpose of this section is to analyze the mechanims involved in the formation of the autoionizing states (Sec. IV A) and to give an interpretation of the main features of the spectra (Sec. IV B).

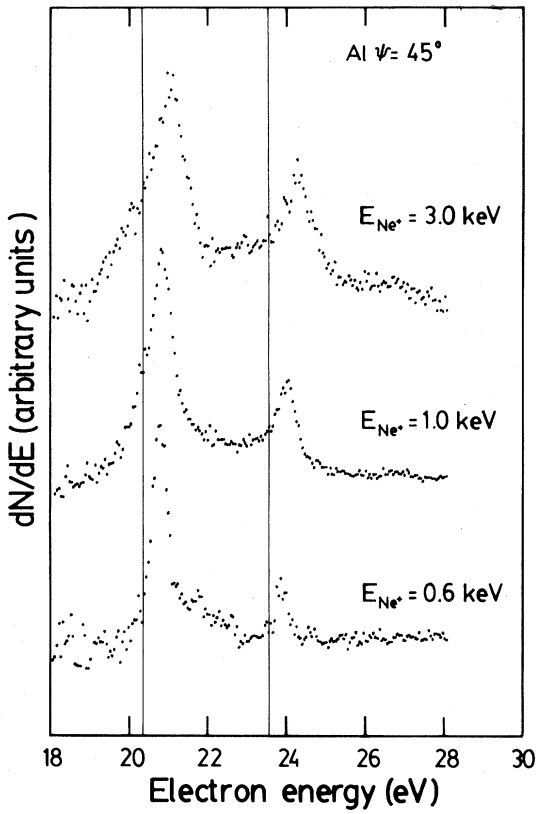

FIG. 6. Electron-energy spectra (after background subtraction) from collisions of 0.6-, 1.0-, and 3.0-keV Ne^+ with Al surfaces. Incidence angle $\psi=45°$. Light vertical lines indicate the energies of autoionization in free space.

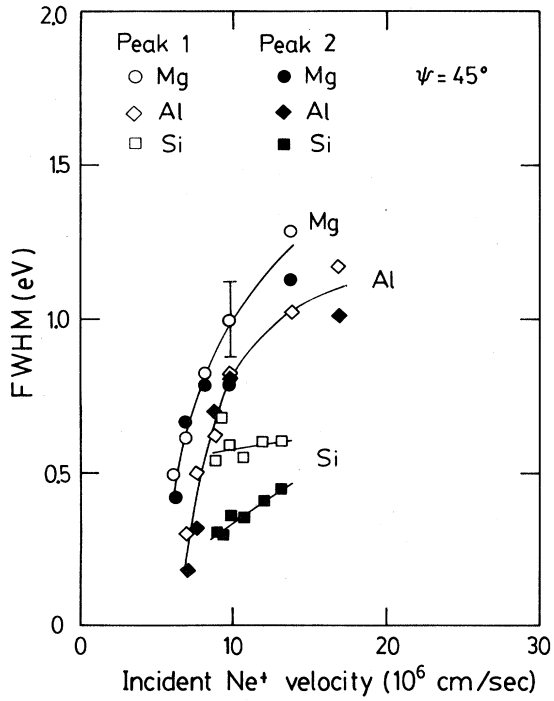

FIG. 7. FWHM vs the incident Ne^+ velocity. Incidence angle $\psi=45°$. Lines are drawn to guide the eye and have no other meaning.

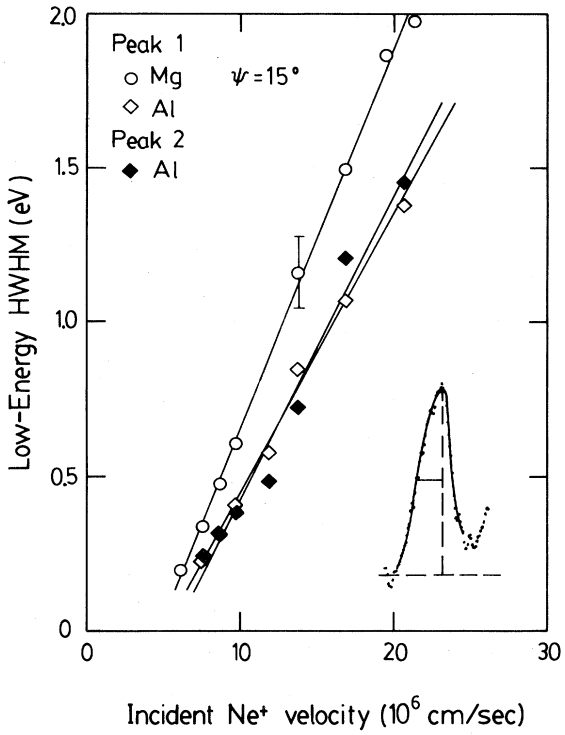

FIG. 8. Low-energy HWHM vs the incident Ne^+ velocity. Incidence angle $\psi=15°$. Lines correspond to the best linear fit. The HWHM is sketched in the inset.

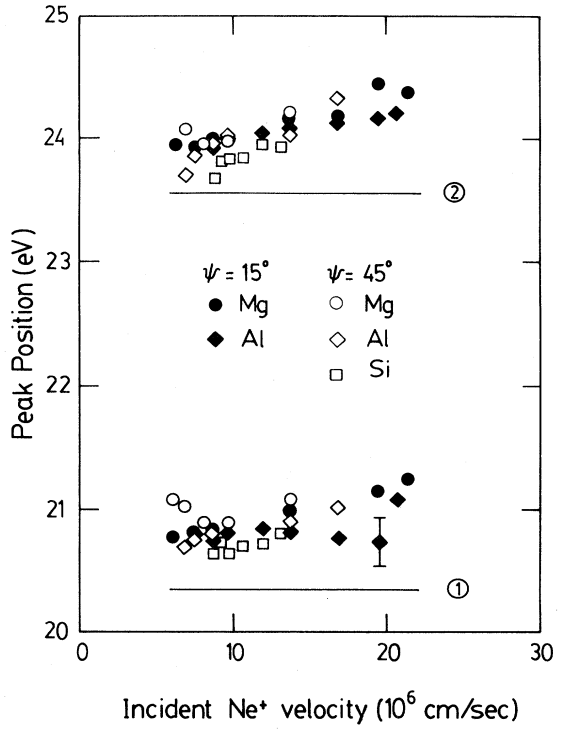

FIG. 9. Most probable energy of autoionization peaks 1 and 2 vs the incident Ne^+ velocity. Energies of autoionization in free space are indicated by the light horizontal lines.

A. Formation of the autoionizing states

It is commonly accepted that the reflection of low-energy heavy ions at surfaces can be described in terms of binary collisions.[6] Furthermore, the atomiclike nature of the inner-shell electrons in the target atoms and the range of Ne^+ velocities used, allow us to analyze our results in the frame of the electron-promotion model.[7] To apply this model it is important to assess the actual charge state of the projectile at the moment of the collision. Hagstrum's theory of Auger neutralization[8] (AN) predicts that practically every incoming Ne^+ is neutralized to the ground state before reaching the surface. We have checked this prediction by measuring the electron-energy spectrum from collisions of 1-keV neutral Ne with Mg ($\psi=45°$). Figure 10 compares this spectrum with that obtained with Ne^+ ions; the agreement at and above the electron energies of peaks 1 and 2 is strong evidence for the neutralization of Ne^+ (the difference between the spectra at low electron energies is due to potential electron emission[8] present for Ne^+ but not for neutral Ne).

In order to ease a comparison of our spectra with those from gas-phase collisions, we review briefly the main characteristics of the latter. The diabatic correlation diagram for the system Ne-Mg is shown in Fig. 11. It is observed that Ne-2p electrons are promoted via the $4f\sigma$ and $3d\pi$ molecular orbitals (MO's). In the first case ($4f\sigma$ MO), the promotion is stronger and many crossings with empty levels occur in a narrow range of internuclear distances. On the other hand, the excitation of electrons of the $3d\pi$ MO is unlikely, since this requires distances of closest approach much shorter than those occurring in these low-energy experiments. Since the excitation of the $4f\sigma$ electrons leaves a neon core $1s^2 2s^2 2p^4$ in a singlet spin state, the spectra from gas-phase collisions are dominated by the autoionization of Ne** ($2p^4 nln'l'$) with a singlet core state (see Fig. 3).

Very different are the spectra from collisions of Ne^+ with solid targets (Fig. 3). The total number of peaks reduces to two, assigned to Ne** ($2p^4(^3P,^1D)3s^2$); the stronger line corresponds now to an autoionizing state with a triplet core. So, we must add new considerations, inherent to collisions with solid targets, to get a good understanding of our spectra.

To simplify the analysis we divide the whole scattering event in three stages. We emphasize that this division is only heuristic; it is worthy inasmuch as it helps to clarify which physical processes occur and in which order they are thought to proceed. The three stages are the following: (1) The incoming Ne^+ is Auger neutralized to the ground state by an electron from the valence band of the solid. The electrons released in this process are those shown in Fig. 10(c). (2) The neutralized projectile suffers a hard collision with a target atom at the surface. In this collision the projectile is reflected and the two $4f\sigma$ electrons are promoted to excited levels of the quasimolecule. The result of these transitions is the formation of a neon

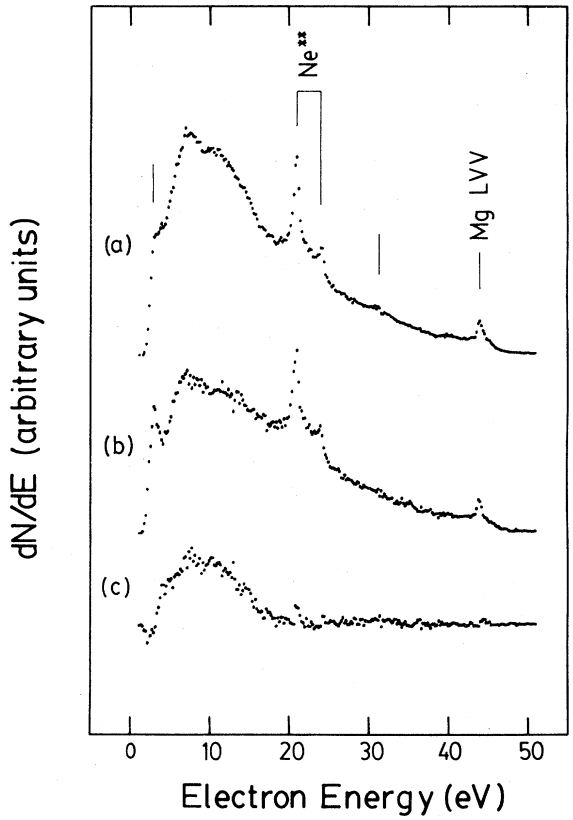

FIG. 10. Electron-energy spectra from collisions of (a) 1-keV Ne^+ and (b) 1-keV neutral Ne with a Mg surface ($\psi=45°$). Spectra are not corrected for the transmission function of the energy analyzer. The Mg LVV Auger line is the reference for normalization. Spectrum (c) is the difference between spectra (a) and (b). For a discussion of the structures at 3 and 31 eV, see the text.

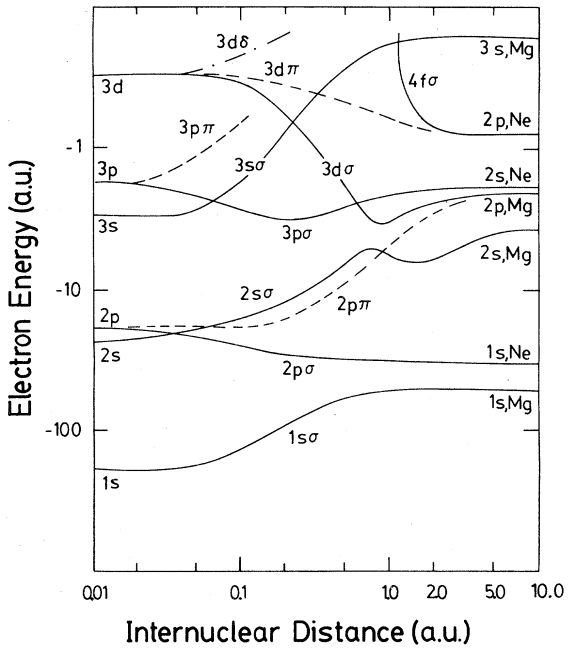

FIG. 11. Diabatic MO correlation diagram for the Ne-Mg system, estimated from that for the Ne-Ne system (Ref. 9).

core in a singlet spin state $1s^2 2s^2 2p^4\,{}^1D$, ${}^1S$. So, to explain the occurrence of the ${}^3P$ core state, we need to postulate (like in atomic collisions in the gas-phase) a core rearrangement process, which is discussed below. (3) The projectile emerges from the "atomic collision" in one of these states

(a) $Ne^{**}(1s^2 2s^2 2p^4 nln'l')$,

(b) $Ne^{+*}(1s^2 2s^2 2p^4 nl)$,

(c) $Ne^{2+}(1s^2 2s^2 2p^4)$,

and again interacts with the surface as a whole. This interaction leads to electronic transitions which either contribute to the formation of the autoionizing states or destroy them. We postulate that the transitions RN (resonant neutralization) and RI (resonant ionization) shown in Fig. 12, being the fastest,[8] occur whenever they are energetically allowed. With this in mind we analyze the evolution of the states (a)—(c) of the reflected projectiles. The autoionizing state (a) is destroyed by RI unless $E_B > W$, where E_B is the binding energy of the outermost electron in Ne**, and W is the work function of the target. State (b), if it survives RI, and state (c) may become autoionizing states after one and two successive RN transitions, respectively. It is seen that the general condition the autoionizing states must satisfy is $E_B > W$. This rule led us in I to the identification of peaks 1 and 2 as corresponding to the states $1s^2 2s^2 2p^4({}^3P, {}^1D)3s^2$, respectively.

A special situation occurs with the Mg target: A projectile emerging from the hard collision as Ne^{2+} cannot reach the intermediate state Ne^{+*} $(1s^2 2s^2 2p^4 3s)$ via RN, and an Auger transition AN (Fig. 12) is required. This transition would release electrons with a maximum kinetic energy of ~ 6 eV and is probably responsible for the 3-eV peak[10] in Fig. 10.

An AN transition filling one of the two $2p$ holes may also occur at any moment during stage (3). This transition, less probable[10] than those just considered for this stage, inhibits the formation of the autoionizing states; the ejected electrons may give rise to the weak structure at 31 eV.

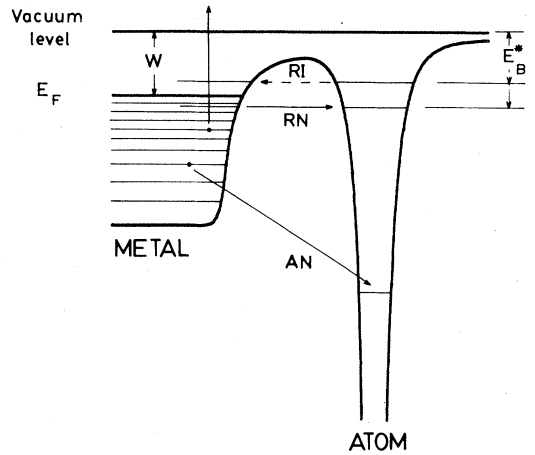

FIG. 12. Auger and resonant processes between an atom (ion) and a metal surface. W is the work function of the metal and E_B^* the binding energy of an excited electronic state of the atom. RI indicates resonant ionization, RN resonant neutralization, and AN Auger neutralization.

Regarding the strong intensity of the autoionizing state with triplet core we attempt an interpretation based on a model proposed by Olsen *et al.*[11] for gas-phase collisions. These authors found that the initial doubly excited molecular states (two vacancies in the $4f\sigma$ MO) can populate doubly excited molecular states (single vacancies in the $3d\pi$ and $4f\sigma$ MO's) which correlate with neon autoionizing states with ${}^3P$ core, via a two-electron rearrangement involving core-Rydberg electron exchange

$$3d\pi^4 nl\sigma n'l'\sigma \rightarrow 3d\pi^3 4f\sigma n''l''\pi n'l'\sigma$$

occurring at a curve crossing.

The extension of this model to the collsion with a metal surface must include, as an essential feature, the continua of occupied and empty electronic states of the target. The net result is that the core rearrangement ${}^1D \rightarrow {}^3P$ should be more probable, since more electrons can participate in the transition (electrons of the valence band can also be excited,[12] in addition to the $4f\sigma$), more empty electronic states are available, and the transition can occur over a wider range of internuclear distances. We should thus expect, in this case, an enhancement in the proportion of autoionizing states with ${}^3P$ core. The increase of the ratio I_2/I_1 with the incident Ne^+ velocity (Fig. 4) supports this model, since the faster the nuclei move, the smaller the probability of the ${}^1D \rightarrow {}^3P$ transition at the crossings. Nevertheless, a calculation of the transition probability is necessary to definitively establish the origin of the state $2p^4({}^3P)3s^2$.[13]

B. Analysis of the spectra

We now turn our attention to the shape of peaks 1 and 2. Since we have assumed that only the reflected projectiles contribute to the peaks in our spectra, the intensity of these peaks should depend on the incidence angle ψ.

A dependence of the intensities on the incidence angle was observed in the case of the Si target. The weak signal appearing at $\psi = 45°$ disappears at $\psi = 65°$. With the Be target, although the diabatic correlation diagram predicts the excitation of Ne autoionizing states, no peak is observed either at $\psi = 45°$ nor at $\psi = 15°$; this is very probably caused by the small reflection of Ne at the surface of Be due to the large mass difference (the maximum Ne^+ scattering angle in a binary collision is $\sim 26°$).

The peak shapes also depend on the incidence angle, as shown in Figs. 5 and 6. We think the differences between these spectra arise from the Doppler broadening of the lines. It is well known that the motion of the electron source produces a shift in the kinetic energy of the ejected electron. Since the velocity of the autoionizing atom (source) is much smaller than the velocity of the ejected electron, we can write

$$K_{\text{lab}} = K_0 + (2mK_0)^{1/2} u_a ,$$

where K_{lab} (K_0) is the electron kinetic energy in the laboratory (autoionizing atom) frame, m is the electron mass, and u_a the velocity of the autoionizing atom in the

analyzer direction (positive when the motion is towards the analyzer). The main differences between the spectra of Figs. 5 and 6 can be understood with this simple formula. To see how these differences come out, let us consider only those collisions where the projectiles reach internuclear distances smaller than that required for the promotion of the two $4f\sigma$ electrons (~ 0.7 Å for Ne-Al). At incident Ne^+ energies smaller than 1.5 keV these projectiles are scattered into angles larger than 45°; so they move towards the analyzer both for $\psi = 45°$ and 15°, and no difference is expected. But at higher impact energies, in the case of $\psi = 15°$, many of these projectiles are scattered into angles smaller than 45° and move away from the analyzer; the electrons ejected from these projectiles are the likely cause for the pronounced broadening of the peaks to the low-energy side (Figs. 5 and 8).

There exist other sources of broadening, besides Doppler, due to the interaction of the autoionizing atom with the surface. We mention some of them without attention to their magnitudes or behavior with ψ:

(i) After autoionization the ejected electon leaves behind the surface polarized by the residual ion; since this polarization amounts to a negative charge, the electron kinetic energy is shifted towards higher energies (this effect probably plays an important role in the shifts observed in Fig. 9).

(ii) The electronic levels of the atom are broadened because of the interaction with the solid.

(iii) The autoionization of the atom may produce shake-up processes in the solid, slowing down the emitted electron.

V. SUMMARY

We have studied the excitation of low-energy Ne^+ projectiles in collisions with solid targets. A comparison of our spectra with those of gas-phase collisions shows close similarities, as the occurrence of doubly excited states of Ne $2p^4nln'l'$, and important differences, like the reduced number of autoionization peaks and the strong intensity of the state $2p^4(^3P)3s^2$.

To interpret our results we postulated a model assuming reflection and excitation of the Ne^+ projectile in its collision with the surface. The excitation mechanism is similar to that of gas-phase collisions, but the continua of occupied and empty electronic states of the target give rise to new features. We have shown that the reduction in the number of peaks is due to the occurrence of resonant transitions of electrons between states in the solid and around the projectile. We also suggested that the continua of electronic states should enhance the formation of the state $2p^4(^3P)3s^2$. The assumption of reflection of the projectiles is supported by the variation of the peak shapes with the incidence angle ψ.

We think this model should remain valid for other projectile–solid-target combinations. This is the subject of present investigations. An important test of the model would be to study the appearance of new peaks when varying the work function of the target.

ACKNOWLEDGMENTS

We acknowledge fruitful discussions with M. M. Jakas, V. H. Ponce, E. V. Alonso, and V. Sidis.

---

*Permanent address: Laboratorium für Festkörperphysik, Eidgenössische Technische Hochschule Zürich, CH-8093 Zürich, Switzerland.

[1]J. Ferrante and S. V. Pepper, Surf. Sci. 57, 420 (1976); C. Benazeth, N. Benazeth, L. Viel, and C. Leonard, C. R. (Paris) B 287, 253 (1978); S. V. Pepper and J. Ferrante, Surf. Sci. 88, L1 (1979); N. Benazeth, C. Leonard, C. Benazeth, L. Viel, and M. Negré, *ibid.* 97, 171 (1980).

[2]G. E. Zampieri and R. A. Baragiola, Surf. Sci. 114, L15 (1982).

[3]R. A. Baragiola, Springer Ser. Chem. Phys. 17, 38 (1981).

[4]H. B. Michaelson, J. Appl. Phys. 48, 4729 (1977).

[5]J. Ø. Olsen and N. Andersen, J. Phys. B 10, 101 (1977); N. Andersen and J. Ø. Olsen, *ibid.* 10, L719 (1977).

[6]W. Heiland and E. Taglauer, Nucl. Instrum. Methods. 132, 535 (1976).

[7]M. Barat and W. Lichten, Phys. Rev. A 6, 211 (1972).

[8]H. D. Hagstrum, in *Inelastic Ion-Surface Collisions,* edited by N. H. Tolk, J. C. Tully, W. Heiland, and C. W. White (Academic, New York, 1973), p. 1.

[9]N. Stolterfoht, in *Structure and Collisions of Ions and Atoms,* edited by I. A. Sellin (Springer, Berlin, 1978), p. 155.

[10]P. Varga, W. Hofer, and H. Winter, Surf. Sci. 117, 142 (1982).

[11]J. Ø. Olsen, T. Anderson, M. Barat, Ch. Courbin-Gaussorgues, V. Sidis, J. Pommier, J. Agusti, N. Andersen, and A. Russek, Phys. Rev. A 19, 1457 (1979).

[12]The excitation of electron-hole pairs by atoms incident on a solid surface has been discussed by, e.g., H. D. Hagstrum, Y. Takeishi, and D. D. Pretzer, Phys. Rev. 139, A526 (1965) and Z. Kirson, R. B. Gerber, and A. Nitzan, Surf. Sci. 124, 279 (1983).

[13]The neon core $2p^4(^3P)$ can also be formed in *two* hard collisions with only one $2p$ electron excited in each collision. However, the survival probability of the first $2p$ hole, in the path to the second collision, should be negligibly small, as we found for the incoming Ne^+.